Supporting Information

Temperature-induced Polymorphism in Methyl Stearate

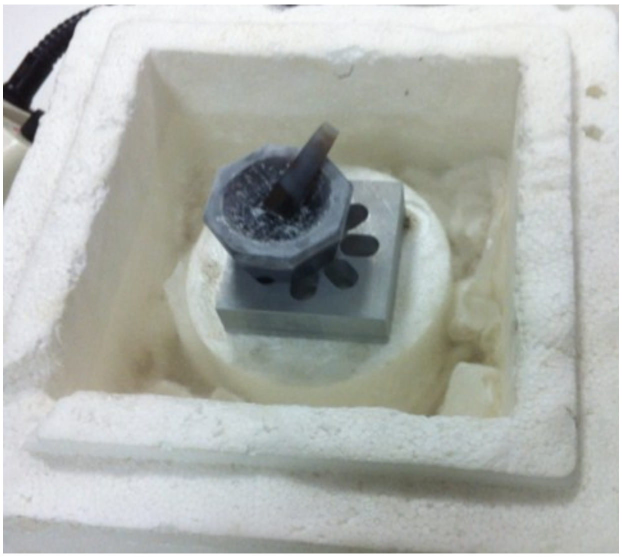

Figure S1. Photograph of a homemade liquid nitrogen bath.

Due to the low melting point of methyl stearate (~38 °C), many factors such as body temperature, the mechanical heat from grinding, and the heat from instruments can affect the powder quality during the sample preparation process. In order to obtain high quality powder samples for XRPD studies and to avoid preferred orientation, a liquid nitrogen bath (**Fig. S1**) was introduced in this work to produce a low-temperature environment. In these studies, a sample of methyl stearate was first melted and then rapidly quenched in a mortar cooled in the liquid-nitrogen bath. The grinding and loading process of the powder sample was also assisted by the liquid nitrogen bath. We used the procedure to produce high-quality powder specimens.

Table S1. Unit cell parameters of Form V of hydrogenous methyl stearate with selected temperatures (synchrotron XRPD data)

T (K)	a (Å)	b (Å)	c (Å)	β(°)	V (Å^3)	R_{wp} (%)
298	49.035(2)	7.397(1)	5.601(8)	77.91(8)	1986.8(6)	4.612
293	49.028(3)	7.387(9)	5.599(5)	77.90(1)	1983.1(4)	4.623
283	49.024(5)	7.369(1)	5.595(6)	77.86(2)	1976.3(1)	4.609
273	49.033(5)	7.350(10)	5.592(5)	77.83(1)	1970.4(6)	4.576
263	49.031(2)	7.330(6)	5.587(7)	77.79(1)	1962.9(6)	4.474
253	49.029(5)	7.312(8)	5.583(9)	77.75(2)	1956.4(8)	4.387
243	49.026(1)	7.295(7)	5.579(8)	77.71(4)	1950.0(6)	4.251
233	49.020(1)	7.281(1)	5.575(9)	77.68(5)	1944.3(4)	4.164
223	49.018(1)	7.265(6)	5.572(1)	77.64(6)	1938.5(3)	4.051
213	49.002(7)	7.250(5)	5.567(3)	77.59(7)	1931.8(8)	4.116
203	49.017(4)	7.237(1)	5.564(2)	77.58(5)	1927.7(2)	3.883
193	49.020(1)	7.224(4)	5.560(7)	77.54(1)	1922.9(2)	4.769

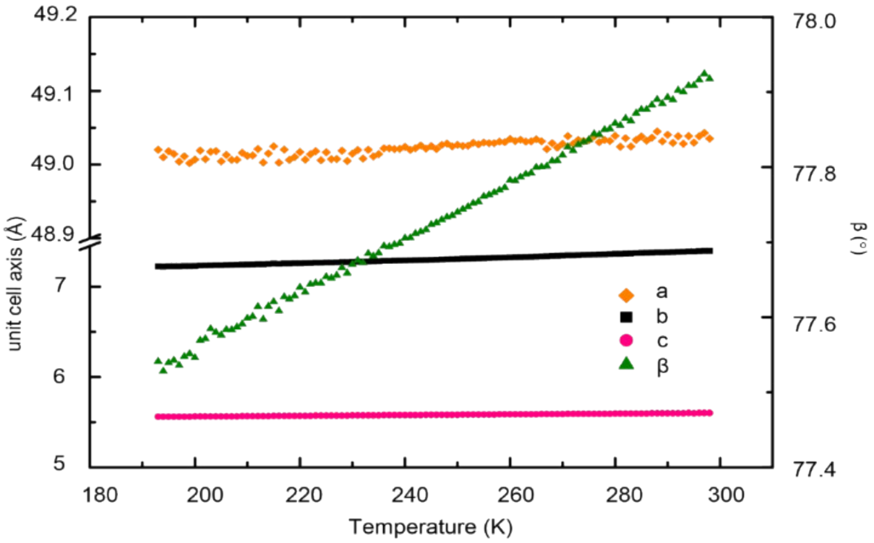

Figure S2. Thermal expansion of the unit cell parameters (a, b, c, and β) of Form V of hydrogenate methyl stearate in the temperature range of 193 K to 298 K, as determined by Rietveld refinement. Data were obtained from synchrotron XRPD.

Table S2. Unit cell parameters of Form V of deuterated methyl stearate with selected temperatures (NPD data)

T (K)	a (Å)	b (Å)	c (Å)	β (°)	V (Å^3)	R_{wp} (%)
4.2	48.906(2)	7.041(4)	5.491(3)	76.954(5)	1842.35(14)	10.56
20	48.905(2)	7.041(3)	5.492(3)	76.954(4)	1842.34(12)	9.664
40	48.909(1)	7.046(3)	5.495(3)	76.989(4)	1845.18(9)	8.954
60	48.910(1)	7.057(3)	5.500(2)	77.041(3)	1850.27(9)	7.853
80	48.914(1)	7.072(2)	5.506(2)	77.094(3)	1856.66(9)	6.651
100	48.917(1)	7.090(2)	5.513(2)	77.152(3)	1864.24(8)	5.42
120	48.921(1)	7.110(3)	5.519(2)	77.210(3)	1872.31(9)	4.611
140	48.927(1)	7.132(2)	5.526(1)	77.275(3)	1881.08(8)	3.608
160	48.933(1)	7.155(2)	5.532(1)	77.343(2)	1890.50(7)	3.253
180	48.937(1)	7.181(2)	5.542(1)	77.414(2)	1900.80(7)	3.081
193	48.947(1)	7.197(4)	5.547(1)	77.456(2)	1907.66(5)	3.414
200	48.946(1)	7.207(2)	5.549(1)	77.480(2)	1911.08(7)	3.124
220	48.949(1)	7.237(2)	5.557(2)	77.549(3)	1922.39(9)	3.567
240	48.955(1)	7.270(3)	5.565(2)	77.630(3)	1935.00(10)	4.466
260	48.961(1)	7.308(4)	5.574(3)	77.706(4)	1948.80(14)	5.616
280	48.965(2)	7.350(5)	5.583(4)	77.790(5)	1964.11(17)	7.467

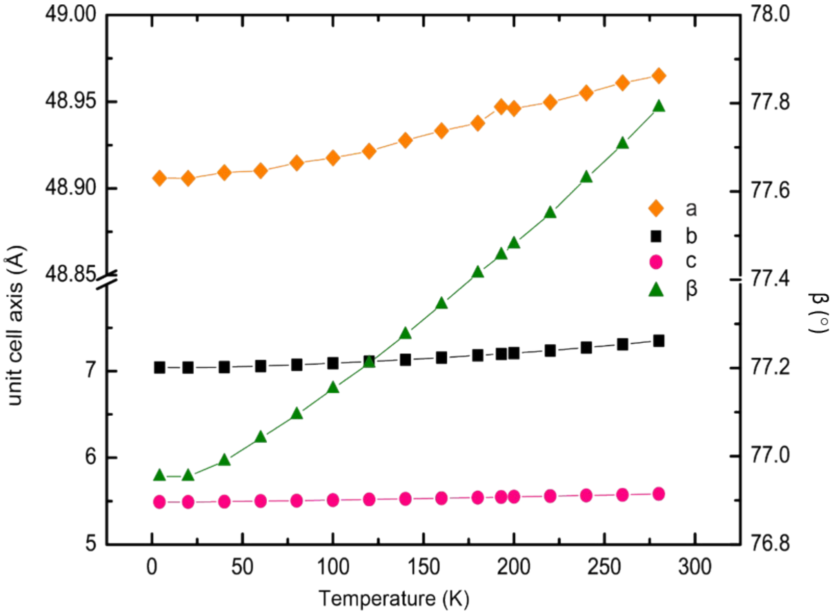

Figure S3. Thermal expansion of the unit cell parameters (*a*, *b*, *c*, and β) of Form V deuterated methyl stearate in the temperature range of 4.2 K to 280 K, as determined by Rietveld refinements from NPD data.

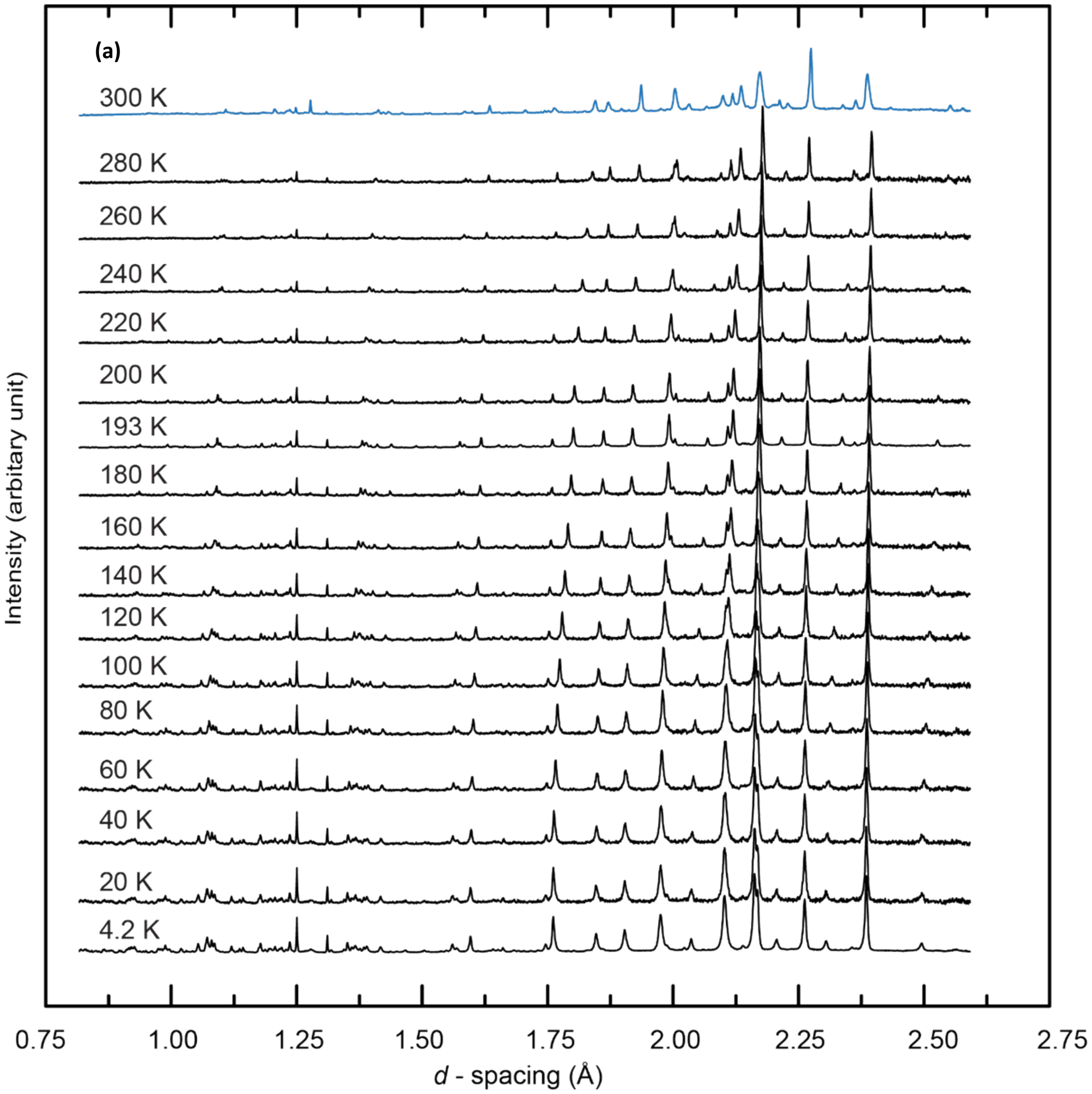
(a)
300 K
280 K
260 K
240 K
220 K
200 K
193 K
180 K
160 K
140 K
120 K
100 K
80 K
60 K
40 K
20 K
4.2 K
Intensity (arbitary unit)
0.75
1.00
1.25
1.50
1.75
2.00
2.25
2.50
2.75
d - spacing (Å)

(a)

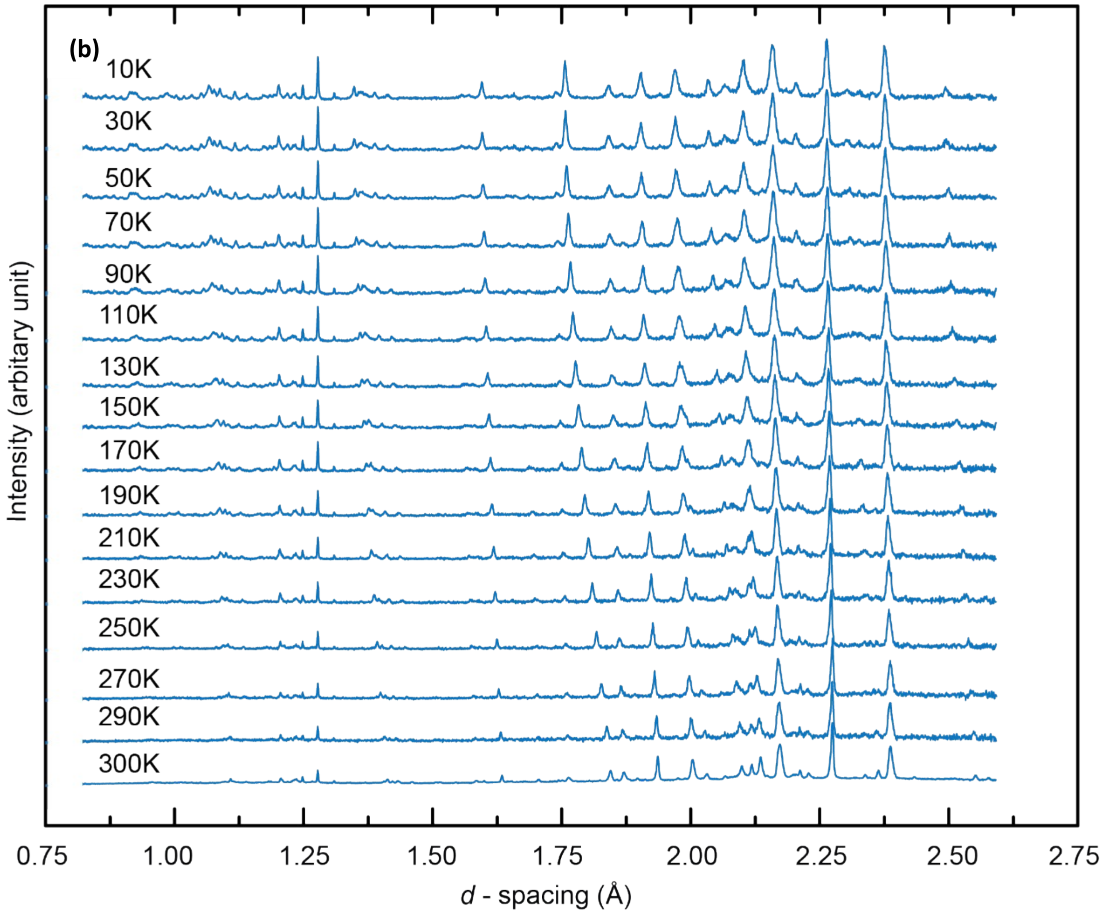

Figure S4. Multiplot of NPD patterns of form V of deuterated methyl stearate collected by the backscattering detector (bank 1) during the variable temperature studies. The patterns collected at 4.2 K, 193 K, and 300 K shown a higher signal-to-noise ratio, due to the longer data collection time (*ca*. 8 h compared to 20 min for other patterns): (a) the patterns collected during temperature increase; (b) the patterns obtained during temperature decrease.

(A)

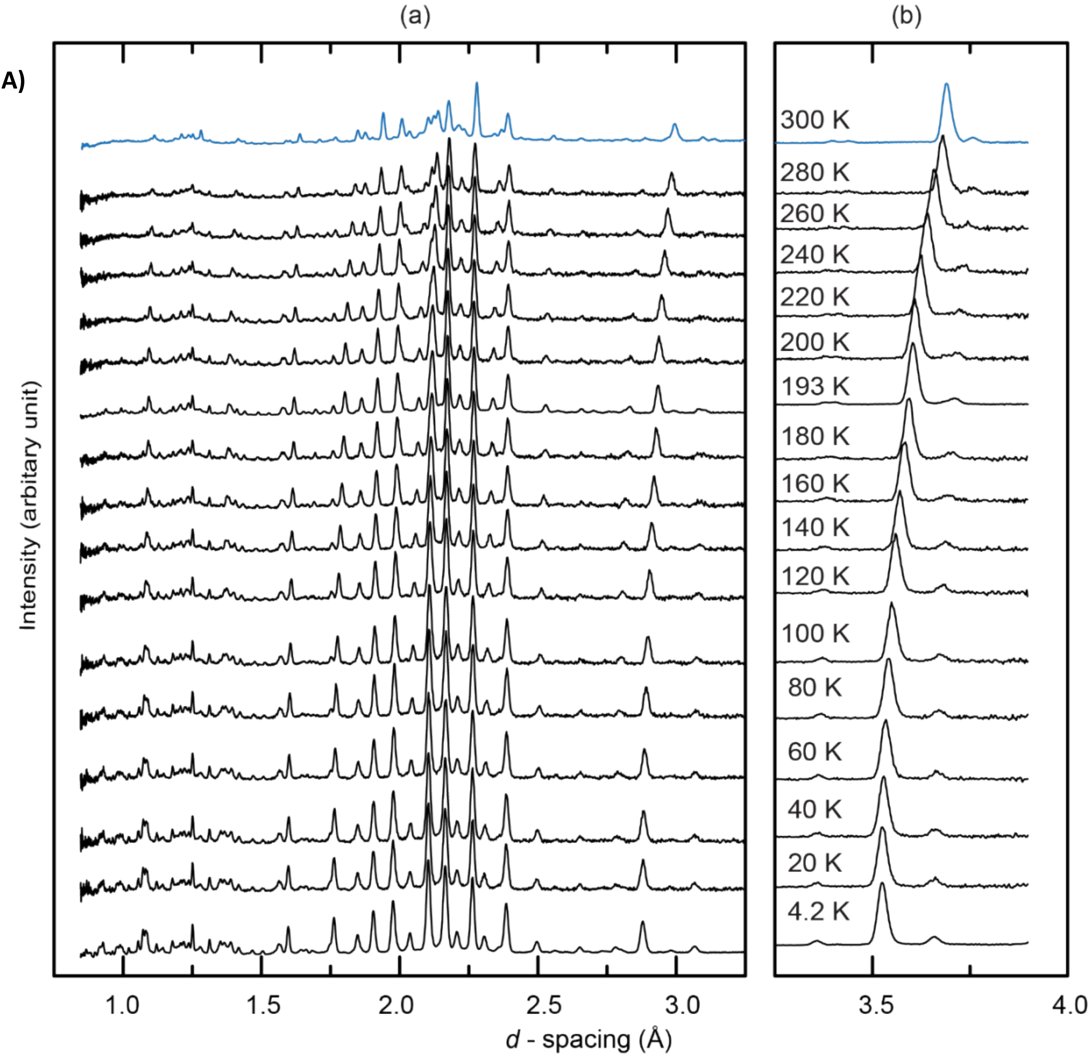
(a)
(b)
Intensity (arbitary unit)
300 K
280 K
260 K
240 K
220 K
200 K
193 K
180 K
160 K
140 K
120 K
100 K
80 K
60 K
40 K
20 K
4.2 K
1.0
1.5
2.0
2.5
3.0
3.5
4.0
d - spacing (Å)

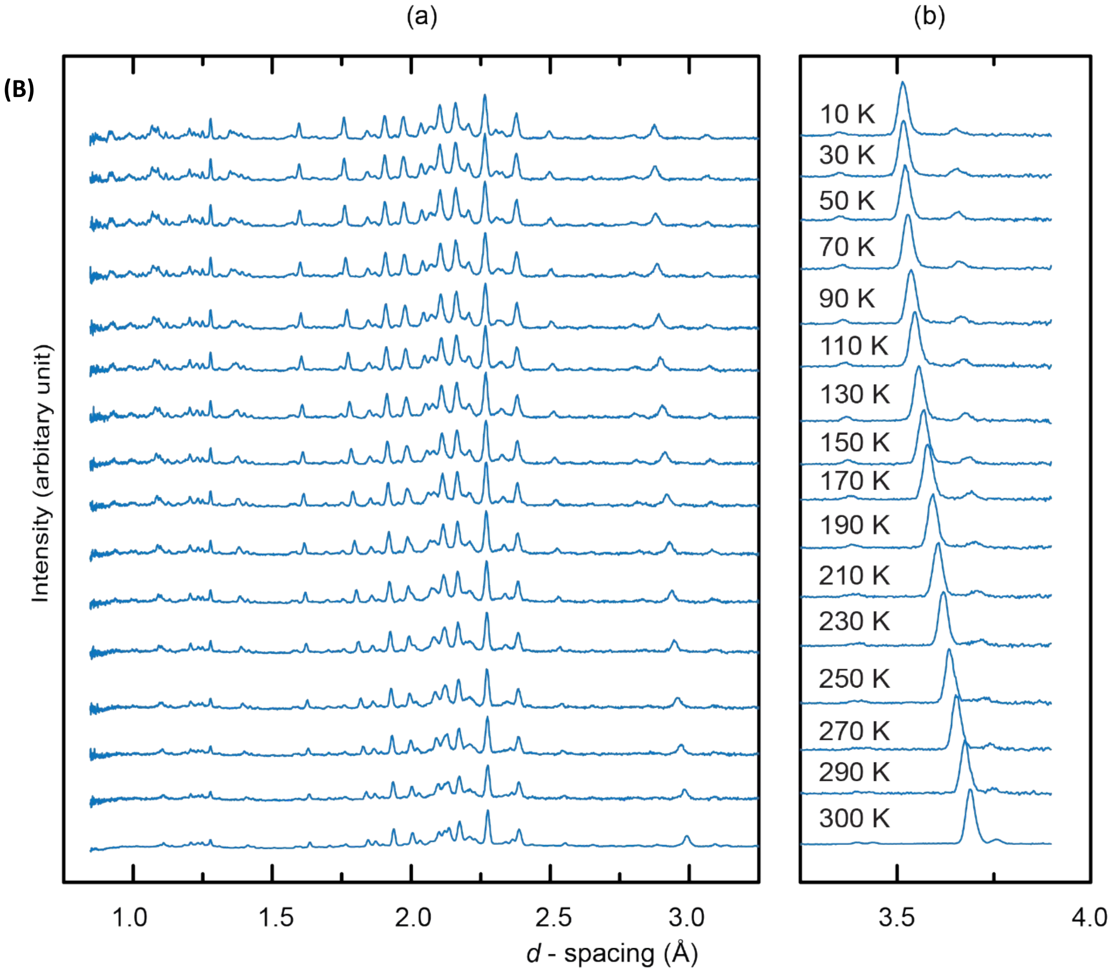

Figure S5. Multiplot of neutron powder diffraction patterns of form V of methyl stearate collected by the complementary detector at 90° (bank 2) during the temperature changes. The patterns collected at 4.2 K, 193 K, and 300 K show a higher signal-to-noise ratio, due to the longer data collection time (circa 8 h compared to 20 min for other patterns): (**A**) the patterns collected during temperature increase; (**B**) the patterns obtained during temperature decrease. The arbitrary unit of **(b)** is 2 times of the unit of **(a).**

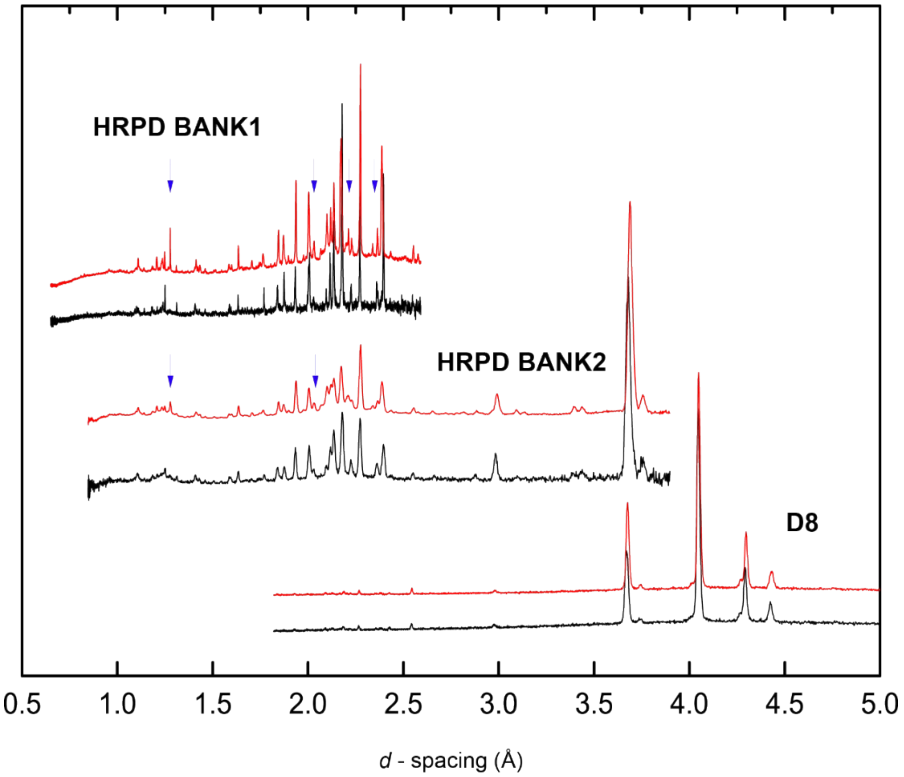

Figure S6. Comparison of XRPD patterns of deuterated methyl stearate collected on the D8-Advanced diffractometer (λ=1.5406 Å) with NPD patterns (bank 1 and bank 2) of the same sample collected on the HRPD instrument: the patterns recorded at 280 K are shown in black, while the patterns obtained at 300 K are shown in red colour. Blue arrows highlight differences induced by phase transition.

The neutron powder diffraction of deuterated methyl stearate collected on HRPD and those recorded on the Bruker D8-Advanced diffractometer are plotted in **Fig. S6**, both before and after the phase transition. All the evidence for phase transitions shown in the high resolution neutron powder diffraction are in the short *d*-spacing range from 1 Å to 2.5 Å, while no clear differences are observed in the *d*-spacing range of 2.5 Å to 4 Å. Due to the limitation of *d*-spacing range which HRPD instrument can reach, the changes of the full NPD pattern of deuterated methyl stearate induced by the phase transition are therefore currently unknown. As a complementary tool, moreover, XRPD patterns of methyl stearate collected on the D8 Lab diffractometer are ambiguous in the *d*-spacing range shorter than 3.5 Å, and no clear evidence of phase transitions in the large *d*-spacing range. This suggests that in the temperature range of 280 K to 300 K, methyl stearate may undergo a second order phase transition, the space group changing from high symmetry to slightly lower symmetry, rather than involving structure reconstruction. Combined with the similarities between the patterns collected on the lab X-ray machine about both hydrogenous and deuterated methyl stearate, it suggests that the second order phase transition from Form V to Form VI is associated with hydrogen atoms. Due to the nature of XRPD, therefore, there will be no evidence shown in the XRPD data.

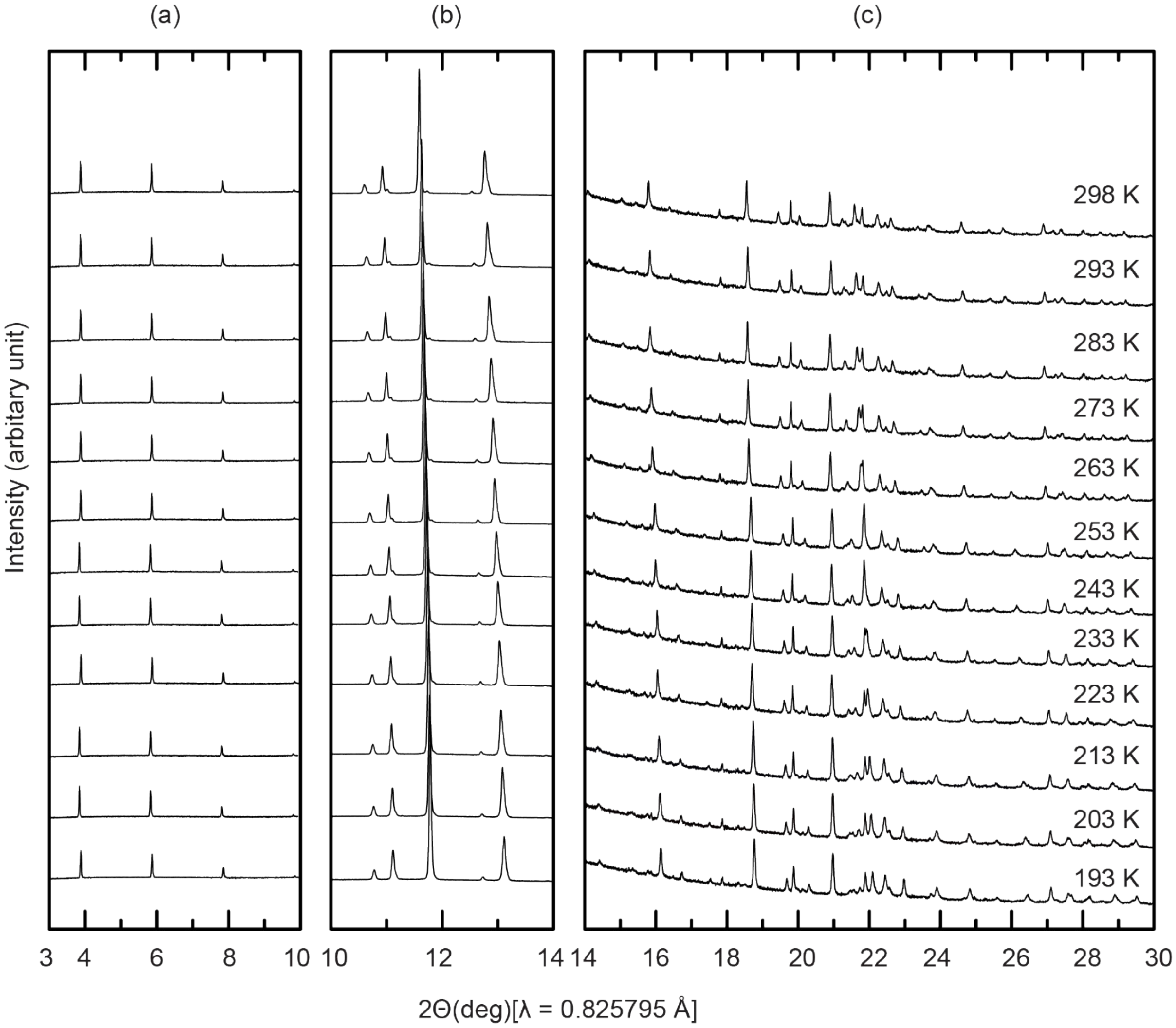

Figure S7. Comparison of synchrotron XRPD patterns of Form V of methyl stearate at selected temperatures. The arbitrary unit of **(b)** is 2 times of the unit of **(a)** and 10 times of the unit of **(c)** for viewing clarity**.**

Table S3. Crystallographic details for methyl stearate from single crystal diffraction methods

Crystallographic form	**Form IV**	**Form III (at 120K)**
Chemical formula	$C_{19}H_{38}O_2$	$C_{19}H_{38}O_2$
M_r (g mol^{-1})	298.49	298.49
Sample preparation methods	Crystallised from pure melt and followed by slow cooling	Crystallised from CS2 supersaturated solution at ~298K
Data collection temperature (K)	120	120
Space group	*C*2/*c*	*Cc*
a (Å)	47.795(13)	95.583(8)
b (Å)	7.1126(17)	7.291(8)
c (Å)	5.5319(15)	5.586(4)
β (°)	90.48(3)	92.57(1)
V (Å^3)	1880.5(9)	3889.6(5)
Crystal shape	Thin plate	Thin plate
Crystal colour	colourless	colourless
Diffractometer	MoKα	CuKα
2θ range of data collection (°)	3.317 – 25.332	7.4 - 152.78
No. of parameters	101	262
No. of reflections	1723	7555
R factors	R_{int} = 0.1576	R_{int} = 0.1416
	R_1 = 0.1160	R_1 = 0.1543
	wR_2= 0.3193	wR_2= 0.4416

The relatively high refinement residuals associated with the single crystal X-ray diffraction model of Form III are a symptom of the problems encountered in growing suitable single crystals – indeed crystals of any quality – of this particular material. Carbon disulfide, for example, is not at all a common solvent for crystallization! The structure is presented in space group *Cc* with two unique molecules in the asymmetric unit. We present in this space group since, despite the correlation of some parameters, it yields a much improved refinement outcome over a centred space group with *Z*' = 1. Two unique molecules in the asymmetric unit better reflects the disordered nature of crystal packing (a model in a centred space group requires whole molecule disorder modelling, which resulted in an unstable and non-converging refinement, even when reasonable restraints were applied). The very long unit cell axis is consistent with the long-chain nature of the molecule. We examined the diffraction pattern to be sure that the *a*-axis had not been artificially doubled by some unidentified twinning but found no such problems and the long axis length appears to be correct. Diffraction was weak, as is typical with long-axis structures, but also consisted of rather streaky Bragg peaks. This is consistent with the waxy nature of the material which is difficult to crystallize and, when crystallized, the crystals were observed to melt at ambient temperature. Copper radiation was used in an attempt to better separate reflections in the reciprocal lattice. Despite all this, and employing various integration options in the CrysAlisPro software, we cannot obtain a data set which gives a refinement outcome any better than that reported in the manuscript. We have restricted our interpretation of the model to gross features, such as molecular torsion, rather than the finer points of bonding details.

Table S4. Crystallographic details for methyl stearate from powder diffraction methods

	Synchrotron XRPD	**NPD**	
Chemical formula	$C_{19}H_{38}O_2$	$C_{19}H_{38}O_2$	
M_r (g mol^{-1})	298.49	298.49	
Crystallographic form	Form V	Form V	
Sample preparation methods	Crystallised from pure melt and followed by flash cooling	Crystallised from pure melt and followed by slow cooling	
Data collection temperature (K)	193	193	
Space group	*Cc*	*Cc*	
a (Å)	49.013(1)	48.947(2)	
b (Å)	7.213(1)	7.198(1)	
c (Å)	5.556(1)	5.547(1)	
β (°)	77.536(2)	77.453(1)	
V (Å^3)	1917.78(7)	1907.60(3)	
Specimen	White powder	White powder	
Diffractometer	I11 (Diamond)	HRPD (ISIS)	
Radiation type	$\lambda = 0.825795(10)$ Å ($2\theta = 0.5° - 29°$)	30-130 ms $2\theta = 168°$	30-130 ms $2\theta = 90°$
No. of data points	7001	3798	1887
No. of parameters	237	985	
R factors	$R_{wp} = 0.09479$	$R_{wp} = 0.0263$	$R_{wp} = 0.0169$
	$R_{exp} = 0.02316$	$R_p = 0.0270$	$R_p = 0.0179$
	$R_{bragg} = 0.02003$	$R_{bragg} = 0.0730$	$R_{bragg} = 0.0944$

Table S6. Interatomic distances and angles for Form V of methyl stearate from synchrotron XRPD

Bond type	Å / °	Bond type	Å / °
C3 - C17	1.64(3)	C19 - C18	1.58(8)
C17 - C13	1.42(2)	C18 - C9	1.52(7)
C13 - C14	1.56(3)	C9 - C12	1.56(8)
C14 - C7	1.58(5)	C12 - C16	1.60(7)
C7 - C15	1.52(8)	C16 - C5	1.52(8)
C15 - C10	1.52(8)	C5 - C4	1.53(8)
C10 - C6	1.52(8)	C4 - C11	1.56(8)
C6 - C8	1.60(7)	C11 - O20	1.15(6)
C8 - C2	1.56(8)	C11 - O21	1.51(6)
C2 - C19	1.45(7)	C1 - O21	1.45(7)
C3 - C17 - C13	109(2)	C2 - C19 - C18	113(5)
C17 - C13 - C14	109(2)	C19 - C18 - C9	113(5)
C13 - C14 - C7	112(3)	C18 - C9 - C12	110(4)
C14 - C7 - C15	114(4)	C9 - C12 - C16	110(4)
C7 - C15 - C10	108(5)	C12 - C16 - C5	114(4)
C15 - C10 - C6	108(5)	C16 - C5 - C4	105(5)
C10 - C6 - C8	109(5)	C5 - C4 - C11	107(5)
C6 - C8 - C2	109(4)	C1 - O21 - C11	112(3)
C8 - C2 - C19	107(5)	C4 - C11 - O20	118(5)
O21 - C11 - O20	118(5)	O21 - C11 - C4	123(4)

Table S7. Interatomic distances and angles for Form V of methyl stearate from NPD

Bond type	Å / °	Bond type	Å / °
C3 - C17	1.36(5)	C19 - C18	1.45(5)
C17 - C13	1.66(5)	C18 - C9	1.58(4)
C13 - C14	1.67(5)	C9 - C12	1.38(5)
C14 - C7	1.57(4)	C12 - C16	1.60(5)
C7 - C15	1.49(4)	C16 - C5	1.62(5)
C15 - C10	1.53(4)	C5 - C4	1.62(5)
C10 - C6	1.50(5)	C4 - C11	1.70(6)
C6 - C8	1.54(4)	C11 - O20	1.30(8)
C8 - C2	1.52(4)	C11 - O21	1.46(8)
C2 - C19	1.53(4)	C1 - O21	1.54(7)
C3 - C17 - C13	95(3)	C2 - C19 - C18	114(3)
C17 - C13 - C14	90(3)	C19 - C18 - C9	124(4)
C13 - C14 - C7	100(3)	C18 - C9 - C12	126(4)
C14 - C7 - C15	114(3)	C9 - C12 - C16	113(4)
C7 - C15 - C10	115(3)	C12 - C16 - C5	109(3)
C15 - C10 - C6	117(3)	C16 - C5 - C4	100(3)
C10 - C6 - C8	112(3)	C5 - C4 - C11	98(3)
C6 - C8 - C2	109(3)	C1 - O21 - C11	116(1)

C8 - C2 - C19	115(3)	C4 - C11 - O20	152(1)
O21 - C11 - O20	111(1)	O21 - C11 - C4	97(4)

Table S8. CCDC deposition numbers for new structures

Name		CCDC deposition numbers
Form III		1589573
Form IV		1811172
Form V	Hydrogenated	1811171
	Deuterated	1811173